# Information Freshness in Random-Access Poisson Network: Average AoI versus Peak AoI

Fangming Zhao*, Xinghua Sun*, Wen Zhan*, Xijun Wang†, Xiang Chen†
*School of Electronics and Communication Engineering, Shenzhen Campus of Sun Yat-sen University, 518107,
†School of Electronics and Information Technology, Sun Yat-sen University, Guangzhou, 510006,
zhaofm@mail2.sysu.edu.cn, {sunxinghua, zhanw6, wangxijun, chenxiang}@mail.sysu.edu.cn

2022 IEEE 96th Vehicular Technology Conference (VTC2022-Fall) | 978-1-6654-5468-1/22/$31.00 ©2022 IEEE | DOI: 10.1109/VTC2022-Fall57202.2022.10012816

***Abstract*—In large-scale wireless networks, severe interference may incur that leads to the age of information (AoI) degradation. It is therefore important to study how to optimize the AoI performance. This paper focuses on the average AoI minimization in random access Poisson networks. By considering the spatiotemporal interactions amongst the transmitters, an expression of the average AoI is derived, based on which the optimal average AoI and the corresponding optimal packet arrival rate and channel access probability are further characterized. We further compare the average AoI optimization with the peak AoI optimization. The comparison reveals that the optimal channel access probability for the average AoI optimization and the peak AoI optimization are the same. Yet, the optimal packet arrival rate for the average AoI optimization is smaller than that for the peak AoI optimization. The gap enlarges when the node deployment density becomes small.**

***Index Terms*—Age of information, Poisson point process, random access.**

## I. Introduction

Information freshness has become an important performance metric in low-latency wireless communication system designing since fresh data is more valuable than stale data for real-time monitoring or control. To assess the timeliness of delivered messages, a novel performance metric, *Age of Information* (AoI), has been put forward in [1] [2]. Age of information is an end-to-end metric that reflects the time elapsed since the last update was generated, and has gained wide attention in both academia and industry.

There have been extensive works on optimizing the AoI performance for wireless networks. [1]–[4] focus on point-to-point communication case. Intuitively, the update packet should be transmitted as soon as possible to obtain better AoI performance. However, by the broadcast nature of the wireless channel, transmitters that share the same spectrum in space would interfere with each other. Then, the high channel access probability for each traffic link would cause severe interference in the network and let the update packet backlog in the queueing system. To understand the AoI performance of wide-area wireless communication networks, [5]–[11] focus on the AoI performance in large-scale networks from the joint perspective of queuing theory and stochastic geometry. A high channel access probability causes more significant aggregate interference and leads to AoI performance degradation. On the other hand, a low channel access probability will also affect AoI performance due to the long waiting time in the queue. For the packet arrival process, the update packet arrives at the system frequently, which will make the update packets stay in the queueing for too long. In comparison, the lower arrival rate leads the terminal information unable to be updated in time and affects AoI performance. Therefore, it is essential to study how to properly tune the packet arrival rate and channel access probability to optimize the AoI performance. The peak AoI performance was studied in [12] for large-scale Poisson networks. Both the explicit expressions of the optimal peak AoI and corresponding parameters are obtained, leaving the average AoI optimization unexplored. In this article, we aim to fill this gap by optimizing the average AoI.

Note that in the existing works, *peak AoI* and *average AoI* are the two key metrics that have been widely used for AoI performance evaluation [3]. The peak AoI is the maximum value of the AoI immediately before an update is received and can be utilized in applications which concerned about the age performance in the worst-case [7], [12]–[14]. The average AoI, on the other hand, denotes the average value of AoI evolution in the whole time horizon, which is often used to evaluate the AoI performance precisely [15]–[18]. Intuitively, the optimal system parameters are distinct towards different AoI optimization objectives. Yet, it remains unknown on how one metric performs when another one is optimized.

To address this issue, this paper derives an expression of the average AoI in the random access Poisson bipolar networks. Individual-optimization and joint-optimization algorithms are further proposed by tuning the packet arrival rate and channel access probability individually or jointly. We compare the average AoI optimization with the peak AoI optimization in [12]. The comparison reveals that the optimal channel access probability for the average AoI optimization and that for peak AoI optimization are the same. Yet, the optimal packet arrival rate for average AoI optimization is smaller than that for peak AoI optimization. The gap enlarges when the node deployment density becomes small.

The remainder of the paper is organized as follows. Section II presents the system model and preliminary analysis. In Section III, the average AoI is derived and optimized by tuning

This work was supported in part by the National Key Research and Development Program of China (2019YFE0114000), in part by the National Natural Science Foundation of China under Grant 62001524, in part by Shenzhen Science and Technology Program (No. 2021A04 and No. RCBS20210706092408010), in part by Guangdong Basic and Applied Basic Research Foundation under grant 2021A1515012631, and in part by Guangdong Engineering Technology Research Center for Integrated Space-Terrestrial Wireless Optical Communication.

978-1-6654-5468-1/22/$31.00 ©2022 IEEE

the channel access probability and the packet arrival rate. Section IV compares the peak AoI optimization and average AoI optimization. Finally, Section V summarizes the work.

## II. System Model and Preliminary Analysis

Consider a mobile D2D network scenario which is modeled as a Poisson bipolar network. Particularly, the network consists of point-to-point links where transmitters are distributed according to a homogeneous Poisson point process (PPP) of density $\lambda$. The corresponding receiver is situated in distance $R$ and oriented at a random direction. Due to the displacement laws in stochastic geometry, the distribution of receivers is also a PPP of density $\lambda$. We consider the high mobility random walk model, where in each time slot, each transmitter is displaced from its initial position to a new position and receivers move accordingly.

On channel modeling, we consider a path-loss exponent $\alpha > 2$ and Rayleigh fading is assumed to characterize the small-scale fading. Each transmission sends the updated information with the same power. Due to all the nodes utilizing the same spectrum for packet delivery, each transmission would be affected by others. Consider a packet is successfully delivered if the received SINR exceeds a decoding threshold $\theta$. Then, the receiver sends an ACK feedback message so that the packet can be moved from the buffer. Otherwise, the receiver sends a NACK feedback message and the packet is retransmitted in the next available time slot until successful. Therefore, the corresponding probability of successful transmission for node $i$ can be written as

$$p_i(t) = P(\mathrm{SINR}_i(t) > \theta). \tag{1}$$

The time is slotted into equal-length intervals, and the transmission of each packet lasts for one slot. The packets arrive at each transmitter following independent Bernoulli processes of mean rate $\xi$. Each transmitter is equipped with a size-one buffer, and hence a newly incoming packet will be dropped if the buffer is full. In each time slot, transmitters with non-empty buffers will access the channel with a fixed channel access probability $q$. If the received SINR exceeds a decoding threshold $\theta$, the packet will send out successfully and queue buffer will be emptied; otherwise, the packet will be retransmitted in the next time slot until success. Then, the dynamics of packet transmissions over each wireless link can be regarded as a Geo/Geo/1/1 queue with the service rate $qp$ and followed FCFS discipline.

We investigate the AoI performance, which captures the timeliness of information delivered at the receiver end. The evolution of AoI $A(t)$ over time for a Geo/Geo/1/1/FCFS queue is illustrated in Fig. 1, where $t_k$ denotes the time slot in which the $k^{th}$ packet arrived, $t_k^{'}$ denotes the time slot in which the $k^{th}$ packet is successfully transmitted, and $t_k^*$ denotes the time slot in which the $k^{th}$ packet is dropped. From this figure, we can see that the AoI $A(t)$ increases linearly over time and plummets at time slots $t_1^{'}, t_2^{'}, t_3^{'}, \ldots, t_n^{'}$ where packets are successfully transmitted. Notably, during the period between $t_2$ and $t_2^{'}$, there is a packet arrivals at slot $t^*$ but is immediately discarded because the buffer can

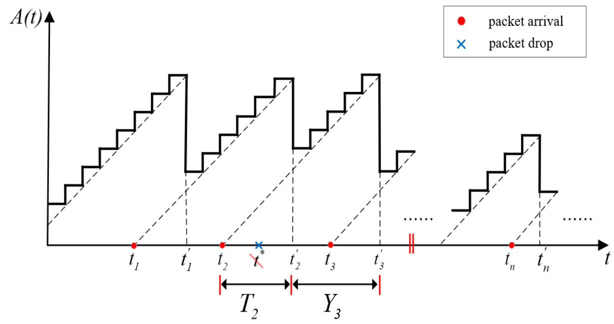


Fig. 1. An example of the AoI evolution over time.

accommodate only one packet. Formally, the progress of such a process can be written as:

$$A(t+1) = \begin{cases} A(t)+1 & \text{transmission failure} \\ t - t_k + 1 & \text{transmission successful.} \end{cases} \tag{2}$$

In this paper, we focus on the average AoI, denoted as $A_{\text{ave}}$, which is defined as the time-average of the entire age process $A(t)$. Such a metric is given by

$$A_{\text{ave}} = \lim_{T\to\infty} \sup \frac{1}{T} \sum_{t=1}^{T} A(t). \tag{3}$$

## III. Optimization of Average AoI

In this section, we first derive an expression of the average AoI in the random-access Poisson network. Based on that, we then optimize the average AoI by tuning the channel access probability $q$ and the packet arrival rate $\xi$.

The probability of successful transmission of a generic transmitter has been obtained in [12] as

$$p = \exp\left\{ -\lambda c R^2 \frac{q\xi}{\xi + pq(1-\xi)} - \theta R^{\alpha} \gamma^{-1} \right\}, \tag{4}$$

where $\alpha$ is the path-loss exponent, $\gamma$ is the SNR at the receiver and $c = \pi\theta^{\frac{2}{\alpha}} / \operatorname{sinc}(\frac{2}{\alpha})$. According to Fig. 1, the $k^{th}$ packet's service time can be expressed as $T_k = t_k^{'} - t_k$, and the inter-departure time between the $(k-1)^{th}$ packet and $k^{th}$ packet can be written as $Y_k = t_k^{'} - t_{k-1}^{'}$. Let $r$ denotes the effective packet arrival rate, the average AoI has been derived in [5] and as

$$A_{\text{ave}} = r\left( \frac{1}{2} E[Y_k^2] + E[T_{k-1} Y_k] + \frac{1}{2} E[Y_k] \right)^{1}. \tag{5}$$

Lemma 1 gives the explicit expression of the average AoI.

**Lemma 1.** *Under the Geo/Geo/1/1 queue assumption with FCFS discipline, the average AoI can be written as*

$$A_{ave} = \frac{2}{qp} + \frac{qp(\frac{1}{\xi} - 1)}{\xi + qp - \xi qp}. \tag{6}$$

*Proof.* See Appendix A □

Lemma 1 shows that the average AoI $A_{\text{ave}}$ is affected by the channel access probability $q$ and the packet arrival rate $\xi$. Consequently, it is of great importance to explore how to

[1]The difference between $+\frac{1}{2}E[Y_k]$ here and $-\frac{1}{2}E[Y_k]$ in [5] is due to the difference in the definitions of initial packet age.

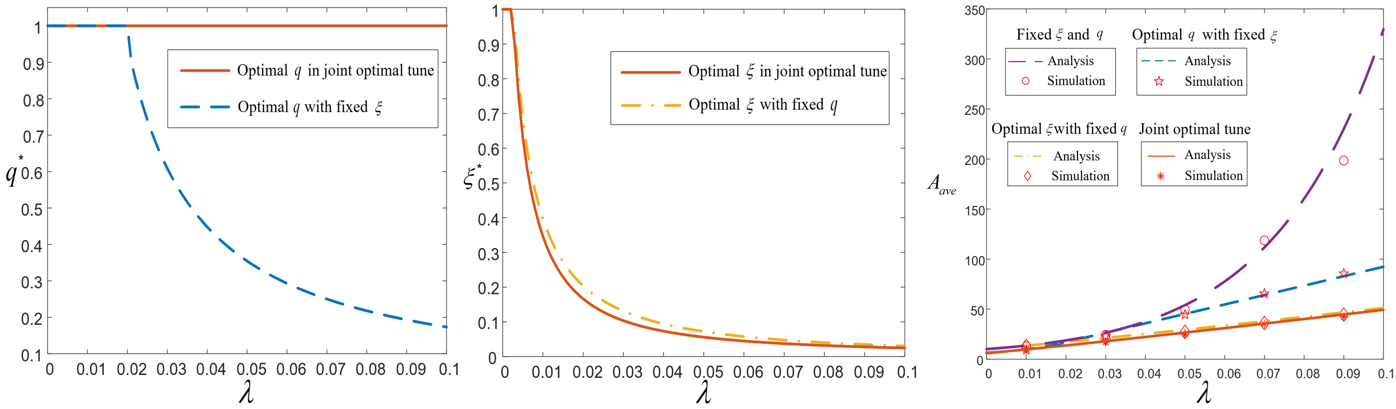


(a) (b) (c)

Fig. 2. (a) $q^*$ in individual and joint optimization (b) $\xi^*$ in individual and joint optimization (c) Average AoI $A_{\text{ave}}$ in fixed parameter, individual optimal tuning the channel access probability with fixed $\xi = 0.5$, individual optimal tuning the channel access probability with fixed $q = 0.6$ and joint optimal tuning. System parameter: Path-loss exponent $\alpha = 3$, decoding threshold $\theta = 0.8$, TX-RX distance $R = 3$, SNR $\gamma = 20$

properly tune the channel access probability $q$ and the packet arrival rate $\xi$ so as to minimize the average AoI $A_{\text{ave}}$, we then formulate the following optimization problem

$$\begin{aligned} A^*_{\text{ave}} = &\min_{\{q,\xi\}} \quad A_{\text{ave}} \\ &\text{s.t.} \quad q \in (0,1], \\ &\qquad\;\; \xi \in (0,1]. \end{aligned} \tag{7}$$

The optimization problem in (7) can be decomposed into two sub-optimization problems: optimal tuning of channel access probability $q$ for a fixed $\xi$, and optimal tuning of the packet arrival rate $\xi$ for a fixed $q$.

### A. Optimal Tuning of Channel Access Probability

The following theorem presents the optimal channel access probability $q^*_\xi$ that minimizes the average AoI $A_{\text{ave}}$, i.e., $A_{\text{ave}}^{q=q^*_\xi} = \min_q A_{\text{ave}}$.

**Theorem 1.** *Given a packet arrival rate $\xi$, the optimal average AoI $A_{ave}^{q=q^*_\xi}$ is given by*

$$A_{ave}^{q=q^*_\xi} = \begin{cases} \frac{2\left(\lambda c R^2 \exp\left\{\theta R^\alpha \gamma^{-1}+1\right\}\right)^2+\frac{1}{\xi}\left(\frac{1}{\xi}-1\right)}{\lambda c R^2 \exp\left\{\theta R^\alpha \gamma^{-1}+1\right\}} - \frac{2}{\xi} + 2 & \\ & \text{if } \lambda c R^2 > 1+\frac{p_*(1-\xi)}{\xi} \\ \frac{2}{p_*}+\frac{p_*\left(\frac{1}{\xi}-1\right)}{\xi+p_*-\xi p_*} & \text{otherwise}, \end{cases} \tag{8}$$

*which is achieved when the channel access probability $q$ is set to be*

$$q^*_\xi = \begin{cases} \frac{1}{\lambda c R^2 - \frac{1-\xi}{\xi}\exp\left\{-\theta R^\alpha \gamma^{-1} - 1\right\}} & \text{if } \lambda c R^2 > 1 + \frac{p_*(1-\xi)}{\xi} \\ 1 & \text{otherwise}, \end{cases} \tag{9}$$

*where $p_*$ is the non-zero root of the following equation*

$$p_* = \exp\left\{-\lambda c R^2 \frac{\xi}{\xi + p_*(1-\xi)} - \theta R^\alpha \gamma^{-1}\right\}. \tag{10}$$

*Proof.* See Appendix B □

Theorem 1 shows that the optimal channel access probability $q^*_\xi = 1$ when $\lambda c R^2 \le 1 + \frac{p_*(1-\xi)}{\xi}$, indicating that in this case, each node would transmit its packet as long as the buffer is nonempty. As the node deployment density $\lambda$, the distance between each TX-RX distance $R$ or the decoding threshold $\theta$ (equivalently, $c$ according to (4)) grows, we have $q^*_\xi < 1$ due to either mounting channel contention or a lower chance of successful packet decoding.

### B. Optimal Tuning of Packet Arrival Rate

The following theorem presents the optimal packet arrival rate $\xi^*_q$ that minimizes the average AoI $A_{\text{ave}}$, i.e., $A_{\text{ave}}^{\xi=\xi^*_q} = \min_\xi A_{\text{ave}}$.

**Theorem 2.** *Given the channel access probability $q$, the optimal packet arrival rate $\xi^*_q$ for minimizing the average AoI $A_{ave}$ is given by*

$$\xi^*_q = \begin{cases} \xi_1 & \text{if } \lambda c R^2 > \frac{\exp\{-\lambda c R^2 q - \theta R^b \gamma^{-1}\}}{2} \\ 1 & \text{otherwise}, \end{cases} \tag{11}$$

*where $\xi_1 \in (0,1)$ is the single root of the following equation*

$$\xi^2 = \frac{qp\left((2-\xi)(1-qp)\xi + qp\right)\left(\lambda c R^2 p \xi (1-\xi) - \left(\frac{\xi}{q} + p(1-\xi)\right)^2\right)}{\lambda c R^2 \left(-2(\xi + pq - \xi pq)^2 + q^2 p^2 (1-\xi)\right)}. \tag{12}$$

*Proof.* See Appendix C □

Theorem 2 reveals that the optimal packet arrival rate $\xi^*_q = 1$ when $\lambda c R^2 < \exp\{-\lambda c R^2 q - \theta R^b \gamma^{-1}\}/2$, indicating that in this case, to minimize the average AoI, new packets shall be updated as frequent as possible. Similarly to Theorem 2, as $\lambda$, $R$, $c$ grows, due to mounting channel contention or a low probability of successful transmission, the optimal packet arrival rate in average AoI optimization $\xi^*_q < 1$.

### C. Joint Optimal-Tuning

So far, we have characterized the optimal tuning of the channel access probability for given packet arrival rate $\xi$, and the optimal tuning of arrival rate $\xi$ for given channel access probability $q$. In this subsection, we will study how to jointly tune the channel access probability $q$ and the arrival rate $\xi$ to optimize the average AoI.

**Algorithm 1** Iterative Algorithm for Calculating $q^*$ and $\xi^*$

1: Input $\lambda$, $R$, $\theta$, $\gamma$, $b$, $\epsilon$
2: Initialize $i=1$, $\xi_i^*$ chosen randomly from (0,1]
3: **repeat**
4: Compute $q_i^*$ based on Theorem 1 and $\xi_i^*$
5: Compute $\hat{A}_{\text{ave}}^{(i)}$ based on $q_i^*$, $\xi_i^*$ and Theorem 1
6: $i \leftarrow i+1$
7: Compute $\xi_i^*$ based on Theorem 2 and $q_{i-1}^*$
8: Compute $\hat{A}_{\text{ave}}^{(i)}$ based on $q_{i-1}^*$, $\xi_i^*$ and (5) and (6)
9: **until** $|\hat{A}_{\text{ave}}^{(i)} - \hat{A}_{\text{ave}}^{(i-1)}| < \epsilon$
10: Let $q^* \leftarrow q_{i-1}^*$, $\xi^* \leftarrow \xi_i^*$ and $A_{\text{ave}}^* \leftarrow \hat{A}_{\text{ave}}^{(i)}$
11: **return** $q^*$, $\xi^*$, $A_{\text{ave}}^*$

Due to the implicit nature of the average AoI, it is hard, if not impossible, to explicitly characterize the optimal channel access probability $q^*$ and the optimal arrival rate $\xi^*$. Instead, based on Theorem 1 and Theorem 2, we propose an iterative algorithm, i.e., Algorithm 1, to obtain $q^*$ and $\xi^*$. Specifically, let $i$ represent the number of iteration, $i \in 1,2,...,$ $q_i^*$ is the channel access probability in $i$th iteration and $\xi_i^*$ is the arrival rate in $i$th iteration. As shown in Algorithm 1, we initialize $\xi_1^*$ by randomly choosing a value from $(0,1]$, based on which and Theorem 1, $q_1^*$ is obtained. With $q_1^*$ and Theorem 2, we can further calculate $\xi_2^*$ and then $q_1^*$, so on and so forth. In each update of either $q_i^*$ or $\xi_i^*$, we compute the corresponding average AoI. The iterations come to an end when the termination condition $|\hat{A}_{\text{ave}}^{(i)} - \hat{A}_{\text{ave}}^{(i-1)}| < \epsilon$ is satisfied, where $\epsilon$ is a small positive number.

### *D. Discussions*

Fig. 2 illustrate how the optimal channel access probability, the optimal packet arrival rate, and the corresponding average AoI vary with the node deployment density. Notably, in Fig. 2(a), we can see that, in the individual tuning, the optimal channel access probability is equal to one when node deployment density is low, and decreases as the node deployment density increases. In joint tuning, the optimal channel access probability is always equal to one.

Fig. 2(b) demonstrates that the optimal packet arrival rate in joint tuning is lower than that in individual tuning, since the optimal channel access rate is equal to one in joint tune. A lower packet arrival rate is thus required to reduce aggregate interference in the network and improve AoI performance.

Fig. 2(c) shows how the average AoI varies with node deployment density in the case of 1) fixed packet arrival rate $\xi$ and channel access probability $q$; 2) optimal-tuning of $q$ for fixed $\xi$; 3) optimal-tuning of $\xi$ for fixed $q$; 4) joint-optimal tuning. We can see that with the fixed packet arrival rate $\xi$ and channel access probability $q$, the average AoI exponentially grows with node deployment density $\lambda$, which is sharply contrasted with that after optimization, which increases linearly with node deployment density $\lambda$. It indicates that the average AoI degrades severely when the nodes deployment density $\lambda$ is large, and careful system parameter tuning is necessary.

## IV. Comparing Peak AoI Optimization and Average AoI Optimization

The peak AoI has been derived in [12], which can be expressed as

$$A_p = E[T_{k-1}] + E[Y_k] = \frac{2}{qp} + \frac{1}{\xi} - 1, \tag{13}$$

and average AoI has been given in lemma 1 and copy as following

$$A_{\text{ave}} = r(\frac{1}{2}E[Y_k^2] + E[T_{k-1}Y_k] + \frac{1}{2}E[Y_k]) = \frac{2}{qp} + \frac{qp(\frac{1}{\xi}-1)}{\xi+qp-\xi qp}. \tag{14}$$

Compared with the peak AoI metric, the average AoI is not only affected by the expectation of service time $\frac{1}{qp}$ and the inter-arrival time $\frac{1}{\xi}$, but also the non-empty probability $\pi_0 = \frac{qp}{\xi+qp-\xi qp}$.

Fig. 3 illustrates that the average AoI and peak AoI vary with the channel access probability and the packet arrival rate by changing the node deploy density. By comparing Theorem 1 in [12] and Theorem 1 in this paper, we find that the optimal channel access probability of optimizing the peak AoI is identical to that for optimizing the average AoI. From Fig. 3(a), we can observe that two metrics could be simultaneously optimized by tuning the channel access probability, when the packet arrival rate $\xi$ is given. In Fig. 3(b), in contrast, it can be observed that the optimal packet arrival rate is different from each other.

We analyze this phenomenon from the perspective of queuing theory. Specifically, according to (6) and (13), both peak AoI and average AoI are sensitive to the service rate. Optimally tuning the channel access probability $q$ benefits the service rate. Therefore, the optimal $q$ for peak AoI optimization and that for average AoI optimization are the same. In contrast to the peak AoI, only the average AoI is sensitive to the non-empty probability. According to (4) and (6), tuning the packet arrival rate $\xi$ would further change the non-empty probability. Therefore, the optimal packet arrival rate $\xi^*$ for peak AoI optimization and that for average AoI optimization might be different.

To take a closer look, Fig. 4 illustrates the difference between the optimal packet arrival rate in peak AoI optimization and average AoI optimization. It can be clearly seen from Fig. 4(a) that the optimal packet arrival rate in peak AoI optimization is larger than that in average AoI optimization. Fig. 4(b) illustrates the optimal parameter in joint optimal-tuning. It can be observed that the optimal channel access probability $q^*=1$ for both the joint optimization of the peak AoI and average AoI. Yet, the optimal packet arrival rate $\xi^{A_p^*}$ to achieve the optimal peak AoI is larger than that in $\xi^{A_{\text{ave}}^*}$. The gap between them decreases as the node deployment density $\lambda$ increases.

## V. Conclusion

This paper focuses on the average AoI minimization in random access Poisson networks. By considering the spatiotemporal interactions amongst the transmitters, an expression of the average AoI is derived. We compare the average AoI

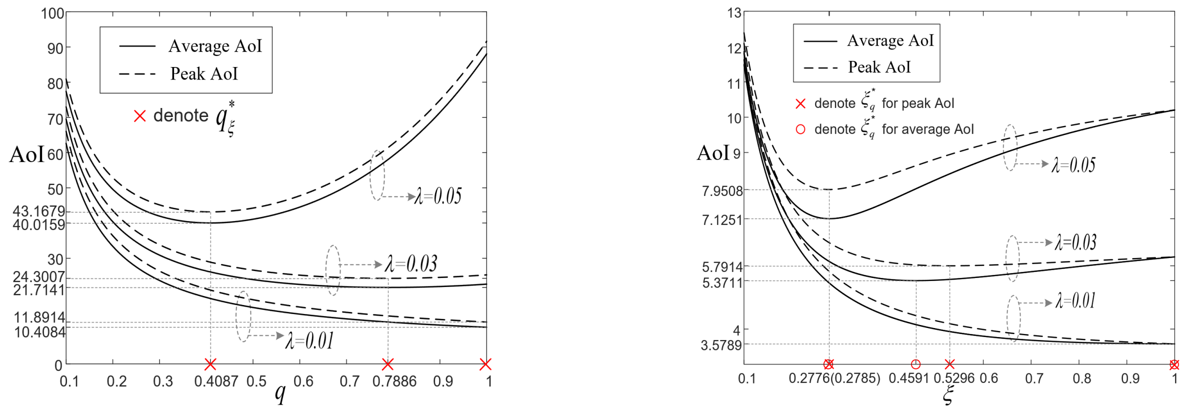


(a) (b)

Fig. 3. Peak AoI and average AoI. System parameter: Path-loss exponent $\alpha = 3$, decoding threshold $\theta = 0.8$, SNR $\gamma = 20$, node deployment density $\lambda \in \{0.01, 0.03, 0.05\}$. (a) AoI versus channel access probability $q$ ($\xi = 0.2$,$R = 3$). (b) AoI versus the packet arrival rate $\xi$ ($q = 1$,$R = 2$).

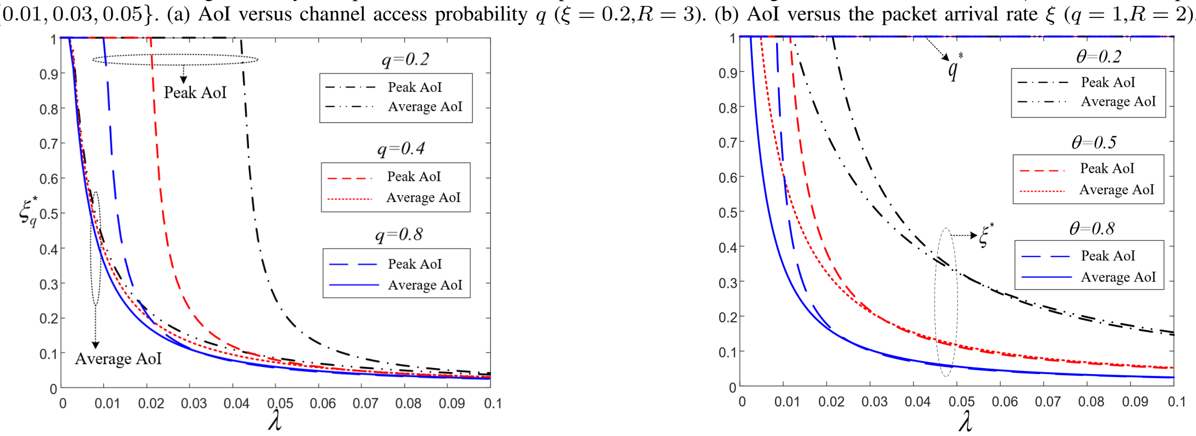


(a) (b)

Fig. 4. Optimal parameter of peak AoI and average AoI. System parameter: Path-loss exponent $\alpha = 3$, decoding threshold $\theta = 0.8$, TX-RX distance $R = 3$, SNR $\gamma = 20$. (a) (Individual optimal) $\xi_q^*$ in average AoI and peak AoI, (b) (Joint optimal) $\xi^*$ and $q^*$ in average and peak AoI.

optimization results with that of the peak AoI optimization in [12]. We find that the average AoI and peak AoI can be optimized simultaneously when individual tuning of the channel access probability. The optimal packet arrival rate might be different from that to minimize the peak AoI. In joint optimization, we design an alternative iterative algorithm by utilizing the results of individual-tuning. Then, we find that the optimal channel access probability is equal to one for both the peak AoI and average AoI. Yet, the optimal packet arrival rate to minimized the average AoI is smaller than that to minimize peak AoI, and the gap diminishes when the node deployment density becomes large.

## Appendix A
## Proof of Lemma 1

In the average AoI i.e., (5), $r$ is the effective arrival rate of Geo/Geo/1/1 queue, which has been derived in [12] as $r = \frac{\xi qp}{\xi+qp-\xi qp}$. $T_k$ is the access delay of $k^{th}$ packet, and is defined as the time spent from the generation of the packet until its successful transmission. The mean access delay given by

$$E[T_{k-1}] = \frac{1}{qp}. \tag{15}$$

$Y_k$ is the sojourn time that the $k^{th}$ packet in the system and can be written as $Y_k = Y_k^a + Y_k^s$, where $Y_k^a$ denotes the time-interval between the departure of $(k-1)^{th}$ packet and the arrival of $k^{th}$ packet, $Y_k^s$ denotes the access delay, then

$$E[Y_k] = E[Y_k^a] + E[Y_k^s] = \tfrac{1}{\xi} - 1 + \tfrac{1}{qp}, \tag{16}$$

$$\begin{aligned} E[Y_k^2] &= E[(Y_k^a)^2] + 2E[Y_k^a]E[Y_k^s] + E[(Y_k^s)^2] \\ &= \left(\tfrac{1-\xi}{\xi^2} + \tfrac{(1-\xi)^2}{\xi^2}\right) + 2\cdot\left(\tfrac{1}{\xi} - 1\right)\cdot\tfrac{1}{qp} + \tfrac{2-qp}{(qp)^2}. \end{aligned} \tag{17}$$

Since $Y_k$ and $T_k$ are independent, we have

$$E[T_{k-1}Y_k] = E[T_{k-1}]E[Y_k] = \tfrac{1}{qp}\cdot\left(\tfrac{1}{\xi} + \tfrac{1}{qp} - 1\right). \tag{18}$$

By submitting (15)-(18) into (5), The explicit expression of average AoI, i.e, (6), can be obtained.

## Appendix B
## Proof of Theorem 1

Based on (6), we have

$$\frac{\partial A_{\text{ave}}}{\partial q} = \left(p + q\frac{\partial p}{\partial q}\right) \times \left(\frac{-2(\xi+qp-\xi qp)^2 + (1-\xi)q^2p^2}{q^2p^2(\xi+qp-\xi qp)^2}\right). \tag{19}$$

In the following, we will show that for $q \in (0,1)$, $\lim_{q\to 0}\frac{\partial A_{\text{ave}}}{\partial q} < 0$, $\lim_{q\to 1}\frac{\partial A_{\text{ave}}}{\partial q} > 0$ for $\lambda c R^2 > 1 + \frac{p_*(1-\xi)}{\xi}$ and $\frac{\partial A_{\text{ave}}}{\partial q} = 0$ has only one non-zero root, implying that the average AoI $A_{\text{ave}}$ first declines and then grows for $q \in (0,1)$ and minimized at the point, which is determined by the root of $\frac{\partial A_{\text{ave}}}{\partial q} = 0$.

First, since $\xi, q, p \in (0,1]$, we have $\xi - \xi qp = \xi(1-qp) > 0$ and the second item of the right side of (19) as

$$\frac{-2(\xi+qp-\xi qp)^2+(1-\xi)q^2p^2}{q^2p^2(\xi+qp-\xi qp)^2} < \frac{-2(qp)^2+(1-\xi)q^2p^2}{q^2p^2(\xi+qp-\xi qp)^2} < 0. \quad (20)$$

We can then only focus on the first item of the right side of (19) because it determines the roots of $\frac{\partial A_{\text{ave}}}{\partial q} = 0$. $\frac{\partial A_{\text{ave}}}{\partial q} = 0$ can be equivalent changed as $\lambda c R^2 = \frac{1}{q} + p\frac{1-\xi}{\xi}$. We denote $f(p) = \frac{1}{q} + p\frac{1-\xi}{\xi} - \lambda c R^2$. It has been shown in [12] that $\frac{\partial p}{\partial q} < 0$ and therefore the derivative in terms of $q$

$$f^{'}(q) = -\frac{1}{q^2} + \frac{\partial p}{\partial q} \cdot \frac{1-\xi}{\xi} < 0, \quad (21)$$

implying that $f(q)$ is a monotonic decreasing function of $q$ for $q \in (0,1]$. Since

$$\lim_{q\to 0} \frac{\partial A_{\text{ave}}}{\partial q} = \lim_{q\to 0} \frac{-2}{q^2 p|_{q\to 0}} = \lim_{q\to 0} \frac{-2}{q^2 \exp\{-\theta R^{\alpha}\gamma^{-1}\}} < 0, \quad (22)$$

and

$$\lim_{q\to 1} \frac{\partial A_{\text{ave}}}{\partial q} = \begin{cases} \lim\limits_{q\to 1} \frac{1}{q} + p\frac{1-\xi}{\xi} - \lambda c R^2 > 0 \\ \qquad\qquad \text{if } \lambda c R^2 > 1 + \frac{p|_{q\to 1}(1-\xi)}{\xi} \\ \lim\limits_{q\to 1} \frac{1}{q} + p\frac{1-\xi}{\xi} - \lambda c R^2 \le 0 \qquad \text{otherwise.} \end{cases} \quad (23)$$

By combining (19)–(23), we show that if $\lambda c R^2 \le 1 + \frac{p|_{q\to 1}(1-\xi)}{\xi}$, then the average AoI $A_{\text{ave}}$ decline for $q \in (0,1]$ and is minimized at $q = 1$. Otherwise, $A_{\text{ave}}$ declines and then grows for $q \in (0,1]$ and minimized at the point, which is determined by the root of $\frac{\partial A_{\text{ave}}}{\partial q} = 0$.

## Appendix C
## Proof of Theorem 2

According to (4) and (6), we have

$$\frac{\partial A_{\text{ave}}}{\partial \xi} = \frac{-qp\xi(2-\xi)(1-qp)-q^2p^2}{\xi^2(\xi+qp-\xi qp)^2} + \Bigg(\Big(-\frac{2}{qp^2} + \frac{q(1-\xi)}{(\xi+qp-\xi qp)^2}\Big) \times \left(\frac{\lambda c R^2 p^2}{\lambda c R^2 p\xi(1-\xi) - (\frac{\xi}{q}+p(1-\xi))^2}\right)\Bigg). \quad (24)$$

$\frac{\partial A_{\text{ave}}}{\partial \xi} = 0$ can be equivalent changed as

$$\frac{1}{\lambda c R^2} = \frac{p\frac{1-\xi}{\xi}}{(\frac{1}{q} + \frac{p(1-\xi)}{\xi})^2} + \frac{\frac{2q\xi^2}{p}(\frac{1}{q} + p\frac{1-\xi}{\xi})^2 - (1-\xi)qp}{((2-\xi)(1-qp) + \frac{qp}{\xi})(\frac{1}{q} + \frac{p(1-\xi)}{\xi})^2} \quad (25)$$

It has been shown in [12] that $\frac{\partial p}{\partial \xi} < 0$. We denote that $g(\xi) = (2-\xi)(1-qp) + \frac{qp}{\xi}$, and derivation of $g(\xi)$ can be written as

$$\begin{aligned} g^{'}(\xi) &= -(1-qp) - \frac{qp}{\xi^2} + q\left(-2+\xi+\frac{1}{\xi}\right)\frac{\partial p}{\partial \xi} \\ &\le -(1-qp) - \frac{qp}{\xi^2} + q\left(-2+2\sqrt{\xi\cdot\frac{1}{\xi}}\right)\frac{\partial p}{\partial \xi} < 0 \end{aligned} \quad (26)$$

Thus, $g(\xi)$ is a monotonic decreases function of $\xi$ for $\xi \in (0,1]$. Then, we denote $t(\xi) = p\frac{1-\xi}{\xi}$, $t(\xi)$ is a monotonic decreases function of $\xi$ for $\xi \in (0,1]$. Then, by combining the rest parts, the right side of (25) is a monotonic increases function of $\xi$ for $\xi \in (0,1]$, and $\frac{1}{\lambda c R^2}$ is a constant value. Thus, $\frac{\partial A_{\text{ave}}}{\partial \xi} = 0$ has one root at most.

Then, by combining (4) and (24), we then have

$$\lim_{\xi\to 0} \frac{\partial A_{\text{ave}}}{\partial \xi} = -\frac{1}{\xi}\left(\frac{1}{\xi} - \lambda c R^2 \frac{1-\exp\{-\theta R^b\gamma^{-1}\}}{\exp\{-2\theta R^b\gamma^{-1}\}}\right) \to -\infty < 0, \quad (27)$$

and when $\lim_{\xi\to 1} \frac{\partial A_{\text{ave}}}{\partial \xi} > 0$, the average AoI $A_{\text{ave}}$ can be optimized for $\xi \in (0,1)$. Combining (24) and (4) , we have

$$\lim_{\xi\to 1} \frac{\partial A_{\text{ave}}}{\partial \xi} = 2\lambda c R^2 q - q\exp\{-\lambda c R^2 q - \theta R^b \gamma^{-1}\}. \quad (28)$$

Thus, similar to the proof in Appendix B, when

$$\lambda c R^2 > \frac{\exp\{-\lambda c R^2 q - \theta R^b\gamma^{-1}\}}{2}, \quad (29)$$

the average AoI $A_{\text{ave}}$ can be optimized for $\xi \in (0,1)$; otherwise, the average AoI $A_{\text{ave}}$ monotonically decreases for $\xi \in (0,1]$. Consequently, Theorem 2 can be obtained.

## References


[1] S. Kaul, R. Yates, and M. Gruteser, "Real-time status: How often should one update?," in *Proc. IEEE INFOCOM, Orlando, FL, USA*, pp. 2731–2735, Mar. 2012.

[2] R. D. Yates and S. Kaul, "Real-time status updating: Multiple sources," in *Proc. IEEE Int. Symp. Inf. Theory (ISIT), Cambridge, MA, USA*, pp. 2666–2670, Jul. 2012.

[3] M. Costa, M. Codreanu, and A. Ephremides, "On the age of information in status update systems with packet management," *IEEE Trans. Inf. Theory*, vol. 62, no. 4, pp. 1897–1910, Apr. 2016.

[4] C. Kam, S. Kompella, G. D. Nguyen, J. E. Wieselthier, and A. Ephremides, "Controlling the age of information: Buffer size, deadline, and packet replacement," in *Proc. IEEE MILCOM, Baltimore, MD, USA*, pp. 301–306, Nov. 2016.

[5] Y. Hu, Y. Zhong, and W. Zhang, "Age of information in poisson networks," in *Proc. Int. Conf. Wireless Commun. Signal Process. (WCSP) Hangzhou, China*, pp. 1–6, Oct. 2018.

[6] H. H. Yang, A. Arafa, T. Q. S. Quek, and H. V. Poor, "Optimizing information freshness in wireless networks: A stochastic geometry approach," *IEEE Trans. Mobile. Comput.*, vol. 20, pp. 2269–2280, Jun. 2021.

[7] M. Emara, H. Elsawy, and G. Bauch, "A spatiotemporal model for peak AoI in uplink IoT networks: Time versus event-triggered traffic," *IEEE Internet of Things J.*, vol. 7, no. 8, pp. 6762–6777, Aug. 2020.

[8] H. H. Yang, A. Arafa, T. Q. S. Quek, and H. V. Poor, "Age of information in random access networks: A spatiotemporal study," in *Proc. IEEE Global Commun. Conf. (GLOBECOM), Taipei, Taiwan*, pp. 1–6, Dec. 2020.

[9] H. H. Yang, C. Xu, X. Wang, D. Feng, and T. Q. S. Quek, "Understanding age of information in large-scale wireless networks," *IEEE Trans. Wireless Commun.*, vol. 20, no. 5, pp. 3196–3210, May 2021.

[10] P. D. Mankar, Z. Chen, M. A. Abd-Elmagid, N. Pappas, and H. S. Dhillon, "Throughput and age of information in a cellular-based iot network," *to appear in IEEE Trans. Wireless Commun.*, 2021.

[11] P. D. Mankar, M. A. Abd-Elmagid, and H. S. Dhillon, "Spatial distribution of the mean peak age of information in wireless networks," *IEEE Trans. Wireless Commun.*, vol. 20, no. 7, pp. 4465–4479, 2021.

[12] X. Sun, F. Zhao, H. H. Yang, W. Zhan, X. Wang, and T. Q. S. Quek, "Optimizing age of information in random-access poisson networks," *to appear in IEEE Internet of Things J.*, 2021.

[13] L. Huang and E. Modiano, "Optimizing age-of-information in a multi-class queueing system," in *Proc. IEEE Int. Symp. Inf. Theory (ISIT), Hong Kong, China*, pp. 1681–1685, 2015.

[14] H. H. Yang, A. Arafa, T. Q. S. Quek, and H. V. Poor, "Locally adaptive scheduling policy for optimizing information freshness in wireless networks," in *proc. IEEE Global Communications Conference (GLOBECOM), Waikoloa, HI, USA*, pp. 1–6, 2019.

[15] I. Kadota, A. Sinha, E. Uysal-Biyikoglu, R. Singh, and E. Modiano, "Scheduling policies for minimizing age of information in broadcast wireless networks," *IEEE/ACM Trans. Networking*, vol. 26, no. 6, pp. 2637–2650, Dec. 2018.

[16] I. Kadota and E. Modiano, "Minimizing the age of information in wireless networks with stochastic arrivals," *IEEE Trans. Mobile Comput.*, vol. 20, no. 3, pp. 1173–1185, Mar. 2021.

[17] B. Zhou and W. Saad, "Joint status sampling and updating for minimizing age of information in the internet of things," *IEEE Trans. Commun.*, vol. 67, no. 11, pp. 7468–7482, Nov. 2019.

[18] J. Sun, Z. Jiang, B. Krishnamachari, S. Zhou, and Z. Niu, "Closed-form whittle's index-enabled random access for timely status update," *IEEE Trans. Commun.*, vol. 68, no. 3, pp. 1538–1551, Mar. 2020.